Supporting Information

Solvent-Assisted Self-Assembly of Gold Nanorods into Hierarchically Organized Plasmonic Mesostructures

Christoph Hanske[1], Eric H. Hill[1,2], David Vila-Liarte[1], Guillermo González-Rubio[1], Cristiano Matricardi[3], Agustín Mihi[3], and Luis M. Liz-Marzán[1,4*]*

[1] CIC biomaGUNE and Ciber-BBN, Paseo de Miramón 182, 20014 Donostia – San Sebastián, Spain

[2] Current address: Institute of Advanced Ceramics, Hamburg University of Technology, 21073 Hamburg, Germany

[3] Institut de Ciència de Materials de Barcelona (ICMAB-CSIC), Campus de la UAB, 08193 Bellaterra, Catalonia, Spain

[4] Ikerbasque, Basque Foundation of Science, 48013 Bilbao, Spain

**corresponding authors: llizmarzan@cicbiomagune.es and christoph.hanske@googlemail.com*

MATERIALS & METHODS

Materials. Hexadecyltrimethylammonium bromide (98%), silver nitrate ($AgNO_3$, ≥99.9%) (5-bromosalicylic acid (90%), L-ascorbic acid (≥99%), sodium borohydride ($NaBH_4$, 99%), (11-mercaptoundecyl)hexa(ethylene glycol) (MUHEG, 90%), isopropanol (IPA, 99.5%) and ethanol (EtOH, 99.8%) were used as received from Sigma-Aldrich. Hydrogen tetrachloroaurate trihydrate ($HAuCl_4 \cdot 3H_2O$, ≥99.9%) from Alfa Aesar was employed without further purification. Polydimethylsiloxane (Sylgard® 184) was purchased as a 2-component kit from Dow Corning. In all experiments Milli-Q® water was used.

Gold Nanorods synthesis and functionalization. Single-crystal gold nanorods with an average length of 55 ± 5 nm and a diameter of 16.5 ± 1.5 nm (aspect ratio: 3.4 ± 0.4) were synthesized *via* a seeded growth method with minor modifications, according to a previously published procedure.[1]

Seeds. The seeds were prepared by the standard CTAB/$NaBH_4$ procedure: 25 μL of a 0.05 M $HAuCl_4$ solution was added to 4.7 mL of a 0.1 M CTAB solution; 300 μL of a freshly prepared 0.01 M $NaBH_4$ solution was then injected under vigorous stirring. Excess borohydride was consumed by ageing the seed solution for 30 min at room temperature prior to use.

Gold nanorods with longitudinal LSPR at 770 nm. In a typical synthesis, 45 mg of 5-bromosalicylic acid was added to 50 mL of 0.05 M CTAB and the mixture was mildly stirred for 15 min until complete dissolution. Then, 480 μL of 0.01 M $AgNO_3$, 500 μL of a 0.05 M $HAuCl_4$ and 200 μL of 0.1 M ascorbic acid solution were added. After 2 h at 25 °C (or once BrSal has completely reduced Au (III) to Au (I), as monitored by the reduction in the absorbance of the Au(III) CTAB complex at 390 nm), 50 μL of 0.1 M ascorbic acid solution and 80 μL of the seed solution were added under vigorous stirring. After 2h, the resulting gold nanorods displayed LSPR maxima in the spectral range of 820 to 890 nm. Tailoring the LSPR to 770 nm was achieved by overgrowth of the synthesized gold nanorods. The amount of ascorbic acid necessary for this was determined by overgrowing small aliquots of the prepared nanorods with increasing volumes of the ascorbic acid solution (0.4 to 0.8 μL per mL). The mixture was left undisturbed at room temperature for at least 4 h before the particles were centrifuge washed for 40 min (7000 rpm, 30 °C) using 50 mM CTAB for redispersion.

F*unctionalization with MUHEG*. The particles were centrifuged again and redispersed in 1 mM CTAB, followed by addition of an equal amount of 200 μM aqueous MUHEG solution under vigorous agitation. After overnight storage, residual ligands were removed by centrifuge washing three times with 250 μM CTAB, whereby the dispersion volume was halved in each step. The cleaned dispersion was finally concentrated up by multiple centrifugation steps to reach to an Au^0 concentration of 1700 mM (according to Abs_{400}).[2] In general, the MUHEG-coated rods could be centrifuged safely with CTAB concentration as low 50 μM. Below that value irreversible particle aggregation started to occur, as corroborated by UV-vis measurements.

Nanoparticle assembly. Dispersions for assembly experiments were always prepared freshly by mixing aliquots of the concentrated stock dispersion with water or CTAB solutions and EtOH in 600 μL centrifuge tubes that were subsequently sealed and stored in the fridge for three days maximum. Due to the extremely high particle concentrations involved and the purposefully induced agglomeration of particles in these dispersions, special care has to be taken to ensure proper dosing and mixing. Mixing by drawing up the liquid in a pipette tip or careful vortexing turned out to be preferable over sonication. Typically, an Au^0 concentration of 100 mM, a CTAB concentration of 100 μM, and an EtOH content of 66% were targeted. Depending on the dimension of the patterned stamp, either 2 μL (for 12 mm^2 total array size) or 4 μL (for 50 mm^2 array size) droplets of these dispersions were placed onto a PDMS stamp, left for a certain time span allowing for EtOH evaporation and particle pre-assembly, and then covered with a clean glass cover slip. The optimal timing for obtaining homogeneous arrays depends on the ambient conditions and dispersion composition, where for the formulation described above, a temperature of approximately 23 °C and a relative humidity around 60% an induction time of 45 - 60 s was found to yield optimal results. Upon complete drying, the glass slide was lifted off and the PDMS stamp cleaned with adhesive tape and IPA. It should be noted that the largest sources of error in this procedure stem from the limited precision of pipetting very small volumes of the viscous, surface active liquids employed and the quick evaporation of EtOH from the stored assembly dispersions. It is therefore advisable to conduct periodic screening experiments checking the time needed for the droplet to develop a golden surface. As a rule of thumb, the target substrate should be applied 5 - 10 s before a bright golden layer starts to grow from the bottom of the droplet toward its apex.

Substrate and mold preparation. As target substrates pieces of standard borosilicate microscopy coverslips (Menzel™, #1.5) cut to 8 x 4 mm^2 (for small molds) or 12 x 12 mm^2 (for larger molds) were used. Cleaning was conducted by rubbing with a 5% Hellmanex™ III solution, sonication in IPA, followed by excessive rinsing with water, and hydrophilization in a UV-O_3 chamber (ProCleaner™) for 30 - 45 min. Soft PDMS molds were replicated by pouring a 10:1 mixture of prepolymer and curing agent either onto patterned silicon masters or OrmoStamp® (Microresist Technology) replica thereof.[3] Degassing the PDMS with vacuum in a desiccator for 2 hours was found to facilitate accurate structure reproduction from the micropatterned molds, which was then followed by curing at 100 °C for at least 45 min. AFM characterization of the employed square patterned molds can be found elsewhere.[4] The following table provides an overview of the pattern dimensions.

Table S1. Stamp Geometries.

Pattern	Lattice Parameter (Center to Center Distance)	Post Diameter
A	20 µm	10 µm
B	1.66 µm	1 µm
C	740 nm	440 nm
D	600 nm	330 nm
E	500 nm	270 nm
F	400 nm	230 nm

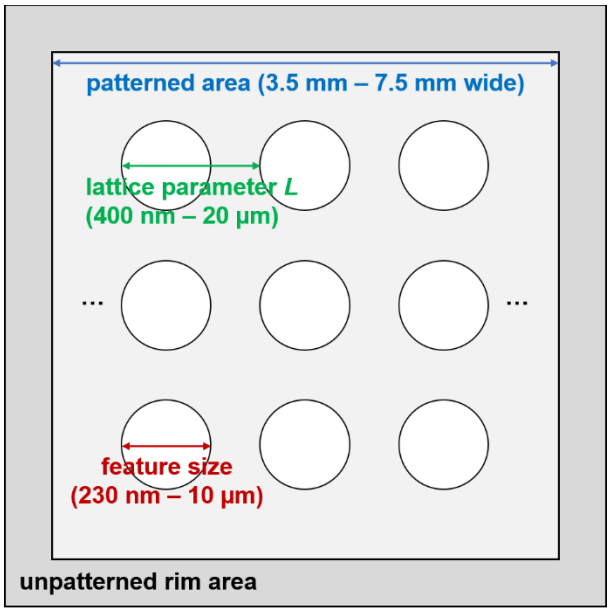

Scheme 1. Sketch of the employed substrate geometries.

UV/vis. Extinction spectra of dilute gold nanorod dispersions were measured using polystyrene cuvettes and an Agilent 8453 spectrometer.

Zeta potential. The zeta potential measurements were conducted with a Malvern Zetasizer Nano ZS. For all measurements in a series the same disposable cuvette was used, intermediate cleaning was done by flushing with EtOH, water, and a particle free solution with otherwise identical composition as the next sample. Zeta potentials were calculated from the electrophoretic mobility values *via* the Smoluchowski equation taking into account the respective solvent compositions.

Scanning electron microscopy. SEM micrographs were recorded on a FEI Quanta 250 operated in low vacuum mode setting (pressure: 100 Pa) or a JEOL JSM-5800 operated in high vacuum mode. Typically, the acceleration voltage was set to to 10 kV and the working distance to 5 mm. The samples were characterized without prior sputter coating.

Transmission electron microscopy. TEM images of the AuNRs were measured with a JEOL JEM-1400PLUS operated at an acceleration voltage of 120 kV. As substrates carbon-coated 400 square mesh copper grids were employed.

AFM imaging. AFM height images were recorded in Tapping Mode™ on a Bruker Multimode V using TESP-V2 cantilevers (f_r: 320 kHz, k: 42 N/m). For data processing the program Gwyddion was employed. First, all elevated areas were marked by hand and excluded from the subsequent line-fitting procedure, which was then followed by background leveling using the three-point plane fitting function and manual correction of the zero setpoint.

Surface-enhanced Raman scattering (SERS) spectroscopy. For SERS measurements a confocal Raman microscope (Renishaw inVia™ Reflex) with a 785 nm diode laser was utilized. The spectra were measured through a 100x objective with an N.A. of 0.9, using a laser power of 1.5 mW and integration times between 0.5 and 5 seconds. As an analyte molecule, bacterial pyocyanin purified *via* chloroform extraction from the supernatant of an 18 hour liquid culture was used diluted either in water or Luria-Bertrani (LB) bacterial growth medium. The substrates coated with plasmonic arrays were cleaned in a two-step procedure comprising a 1 min etching with O_2 (Diener PICO, 200 W, 0.4 mbar) followed by a 30 min UV-O_3 treatment. Subsequently, the substrates were immersed in the test media for at least 30 minutes and then dried under a nitrogen stream. Data acquisition and analysis was conducted using the WIRE™ 4 software.

Molecular Dynamics Simulations. MD simulations and analysis were carried out using GROMACS 5.0.7.[5] The GolP-CHARMM forcefield was used to describe the Au (100) surface and the sulfur atom of MUHEG.[6] The GolP-CHARMM forcefield provides dynamic polarization through the use of a virtual site offset from each gold atom, where each has a partial charge of +0.3 and -0.3, respectively. This provides more accurate depictions of the surface binding interactions of small molecules with the Au surface than other models which rely solely on the use of Lennard-Jones (LJ) terms. The MUHEG and CTA^+ were modeled using the CHARMM36 forcefield.[7] Parameters for the ions were derived from Stillinger *et al.*, and the TIP3P water model was used.[8] Furthermore, the description of the S-Au interaction follows a study by Colangelo *et al.*, where the thiol is modeled as S^-, providing both strong interactions and realistic lateral diffusion of bound surfactants.[9]

Initially, 100 MUHEG molecules were randomly placed in a 3.4 x 3.5 x 5.8 nm box above the Au surface, solvated, and ionized using Na^+. A steepest descent energy minimization

was performed, and following simulations used a 2 fs time step and constraint of bonds between hydrogens and other heavy atoms using the LINCS algorithm.[10] Electrostatic interactions were calculated using the particle mesh Ewald (PME) method of summation with a cutoff value of 1.2 nm.[11] The "v-rescale" thermostat by Bussi, Donadio, and Parrinello was used to maintain a system temperature of 298K.[12] Following energy minimization and NVT equilibration, NPT simulation for 50 ns results in a uniform coating of MUHEG with thiol groups bound to the Au surfaces. The bound MUHEGs are removed from one of the Au surfaces (across the periodic boundary in the Z direction), and MUHEGs which were adsorbed with thiols facing towards the solvent were also removed. Following a further 50 ns NPT simulation to allow for lateral diffusion of the bound MUHEGs, 50 CTAB molecules are added to system and the system is solvated in water and simulated using the NPT ensemble for 100 ns. During this time, the insertion of CTA^+ molecules into the MUHEG layer is observed (**Figure S7**). Finally, excess CTA^+ in the water box is removed, and from this point the system is treated as the surface of a MUHEG-functionalized Au nanorod in a CTAB solution.

This system was then solvated in 1800 water molecules after the addition of 50 or 80 CTAB molecules randomly placed in the box. Simulation using the NPT ensemble leads to the CTAB forming a micelle at the MUHEG interface within the first 10 ns, and over 200 ns of simulation the micelle remains bound at the interface. The output of 200 ns of NPT simulation in water is stripped of water, and then solvated with either 750 ethanols (100% v/v EtOH) or 400 ethanols and 1100 waters (52% v/v EtOH). These systems were each simulated up to 300 ns using the NPT ensemble. Trajectories were visualized using UCSF-Chimera and analysis performed using GROMACS built in packages.[13]

ADDITIONAL CONTENT

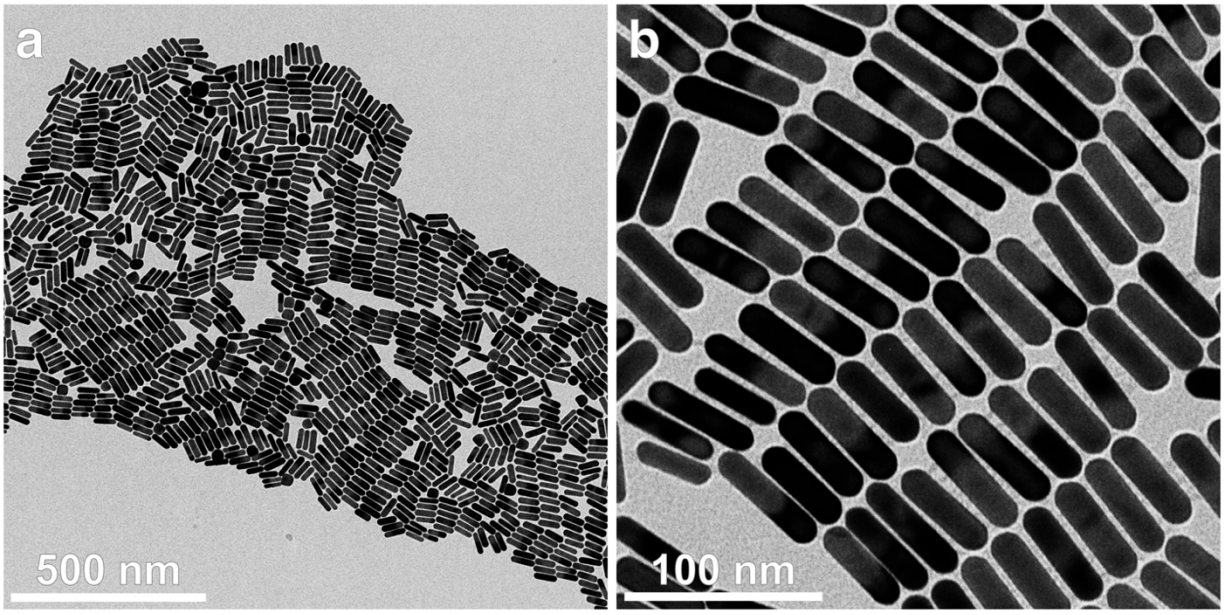

Figure S1. Representative TEM micrographs of the employed AuNRs: overview (a) and close-up (b).

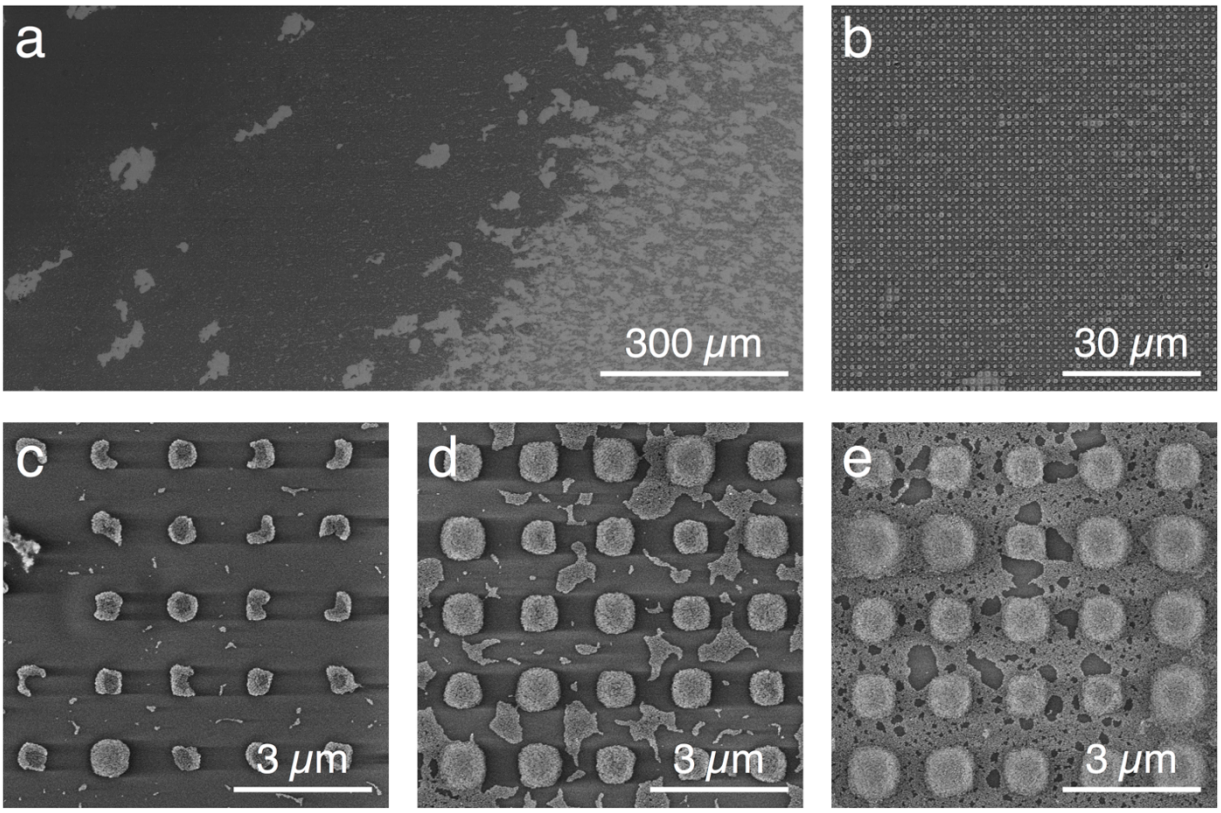

Figure S2. SEM images from a good substrate prepared by assembly of gold nanorods without ethanol in the dispersion medium. Typically, toward the rim of the substrate a strongly overfilled coffee ring builds up, whereas the substrate center remains strongly underfilled or even empty. (a) and (b) show overviews of the substrate at different magnifications. The zoomed images in (c-e) were taken with the same magnification at different spots.

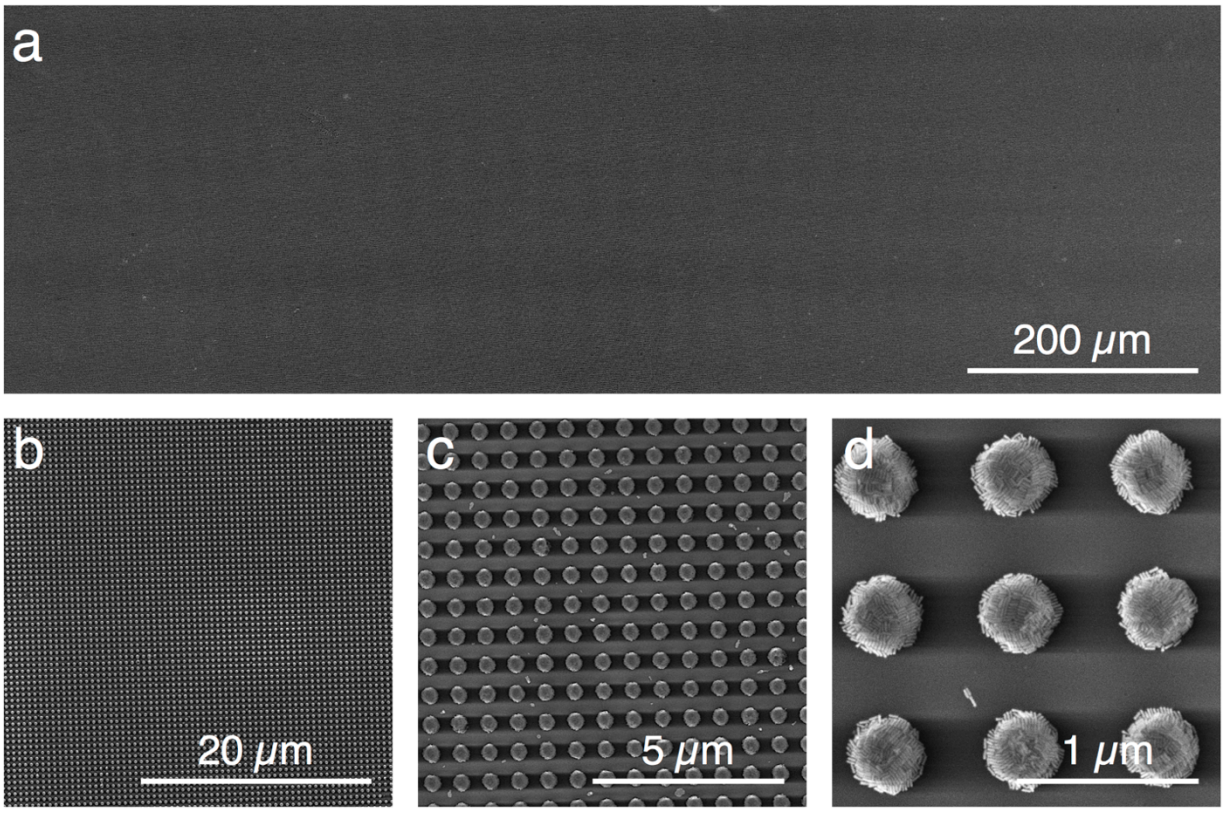

Figure S3. SEM images from a typical substrate prepared by assembly of gold nanorods from a dispersion containing ethanol as the main component under optimized conditions. Over the entire sample homogeneous rod arrays and accurate reproduction of the stamp geometry were obtained. The micrograph in (a) provides an overview of a macroscopic area, whereas (b-d) are close-ups of the same spot recorded with increasing magnification.

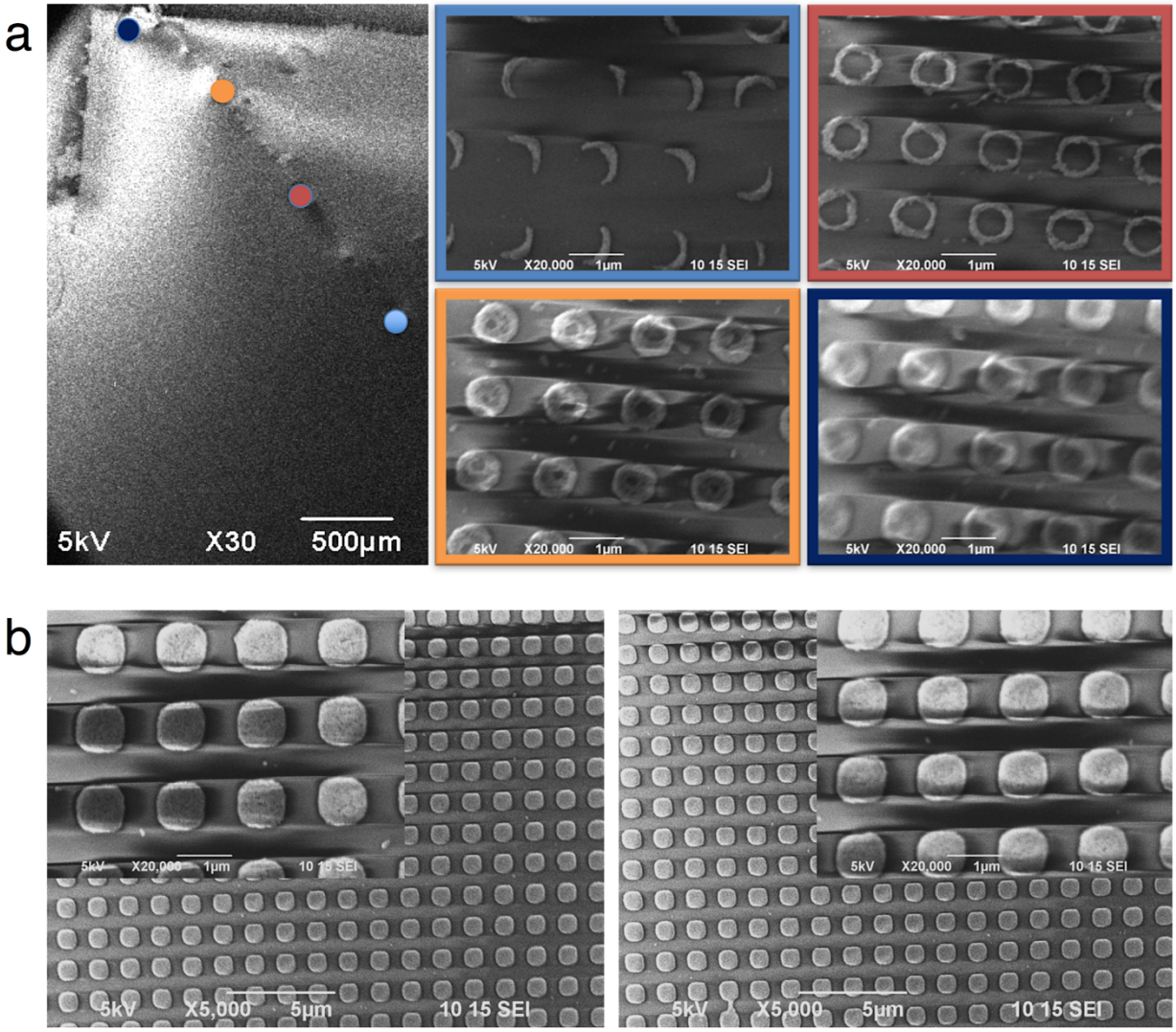

Figure S4. Kinetic study: microscopic investigation of substrate homogeneity for short (a) and long waiting times (b) before substrate application onto an EtOH containing dispersion droplet. Covering the evaporating droplet immediately with a glass cover slip still results in particle accumulation at the substrate edge despite the presence of the volatile solvent (a). A longer period of solvent evaporation preceding substrate application clearly improves the obtained macroscopic and local homogeneity removing differences between center (b, left) and rim (b, right) region.

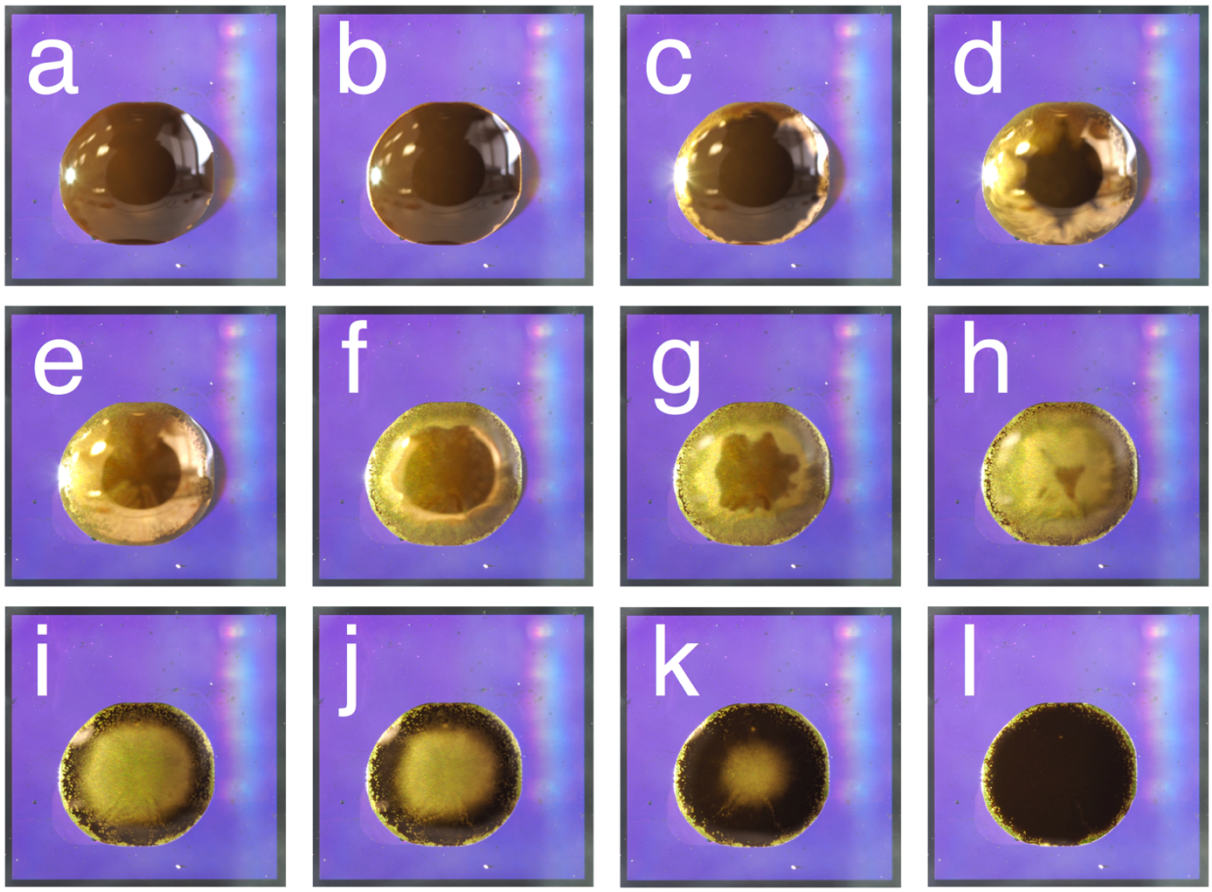

Figure S5. Macrophotos of an evaporating dispersion droplet sitting on a microstructured PDMS stamp after different waiting times. The initially brown AuNR dispersion (100 mM Au^0, 75% EtOH v/v) (a) first begins to accumulate particle agglomerates at the rim (b) due to a higher evaporation rate attributed to the locally increased droplet curvature. The golden surface layer grows from the bottom to the top (c,d) eventually covering the entire liquid-air interface (e). After several minutes of waiting, during which more particles accumulate (f-h) the largest fraction of ethanol has evaporated and the particles start to redisperse partially near the rim (i-l). The first frame (a) was taken approximately 25 s after droplet applications, (b): 34 s, c: 40 s, d: 45 s, e: 53 s, f: 108 s, g: 127 s, h: 147 s, i: 194 s, j: 210 s, k: 238 s, l: 297 s. The dark area visible in the center of the images (a-f) is the reflection of the camera objective.

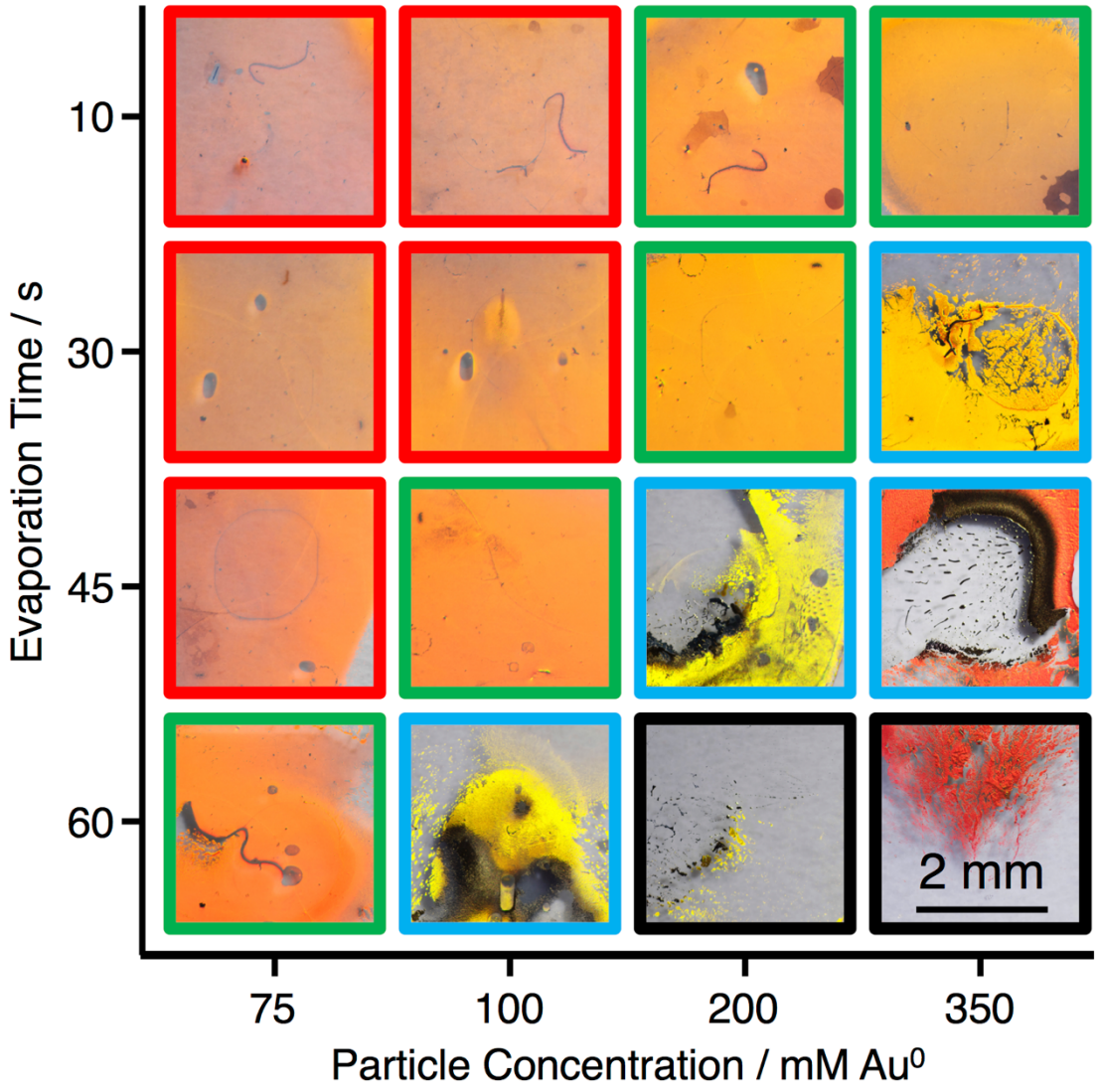

Figure S6. Influence of particle concentration and evaporation time on the final substrate homogeneity documented by macrophotos for a fixed CTAB concentration of 100 µM. Both parameters have a similar influence on the resulting repartition of nanoparticles over the surface suggesting that the degree of particle agglomeration at the moment of substrate application determines the final outcome. Substrates with homogeneous arrays covering more than 50% of the total treated area are marked with a green frame. The remaining imperfections visible in these samples are mainly attributable to enclosed air bubbles and scratches on the PDMS stamps. Variations of the diffractive colors between the samples stem from the use of stamps with slightly different periodicities ranging from 1.00 to 1.14 µm.

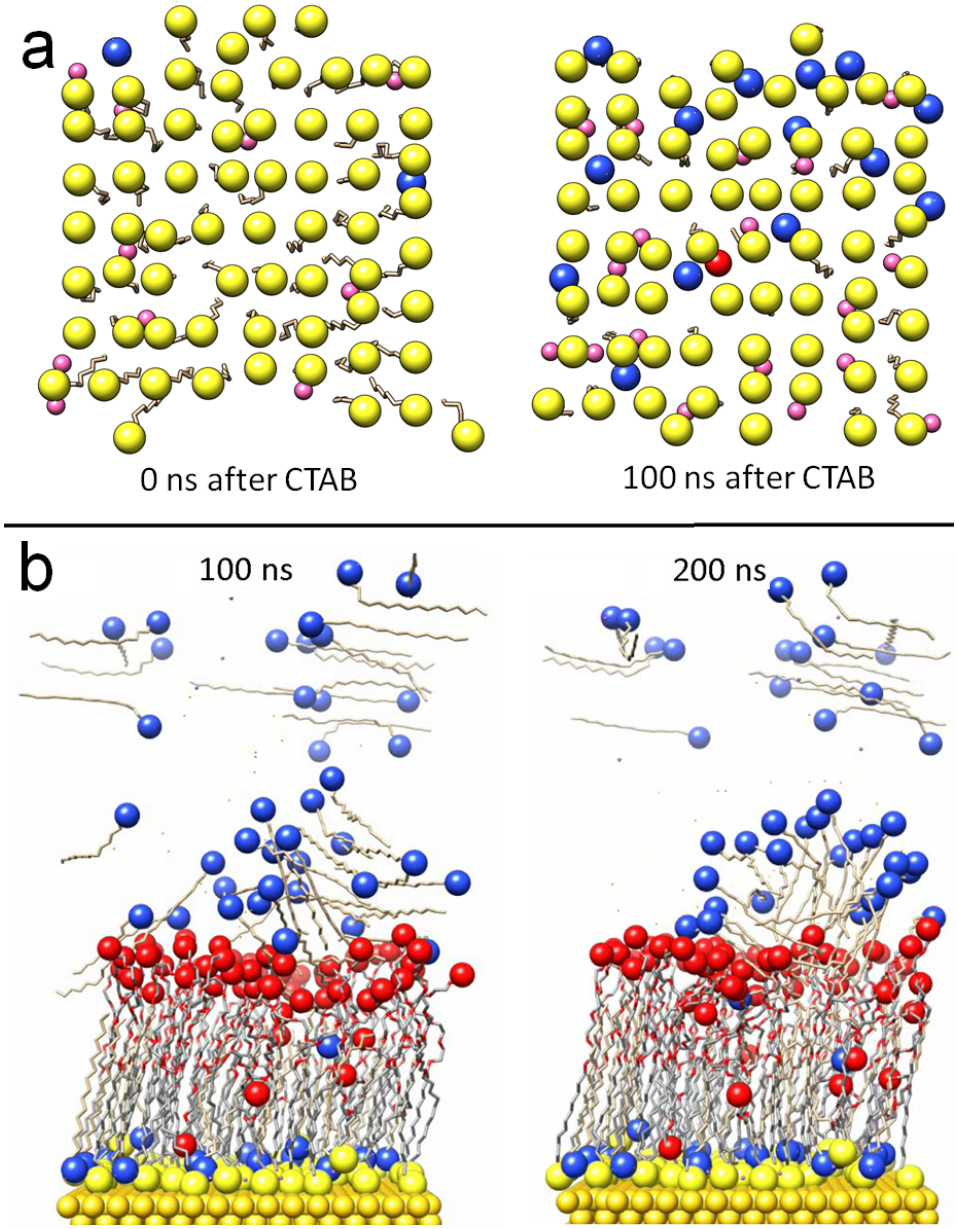

Figure S7. (a) Equilibration of MUHEG layer with CTAB to prepare initial configuration, before and after 100 ns of simulation using NPT ensemble. (b) Simulation results in pure water after 100 ns (left) and 200 ns (right). In absence of ethanol, the loose CTA^+ micelle stays bound at the MUHEG interface over the entire simulation trajectory.

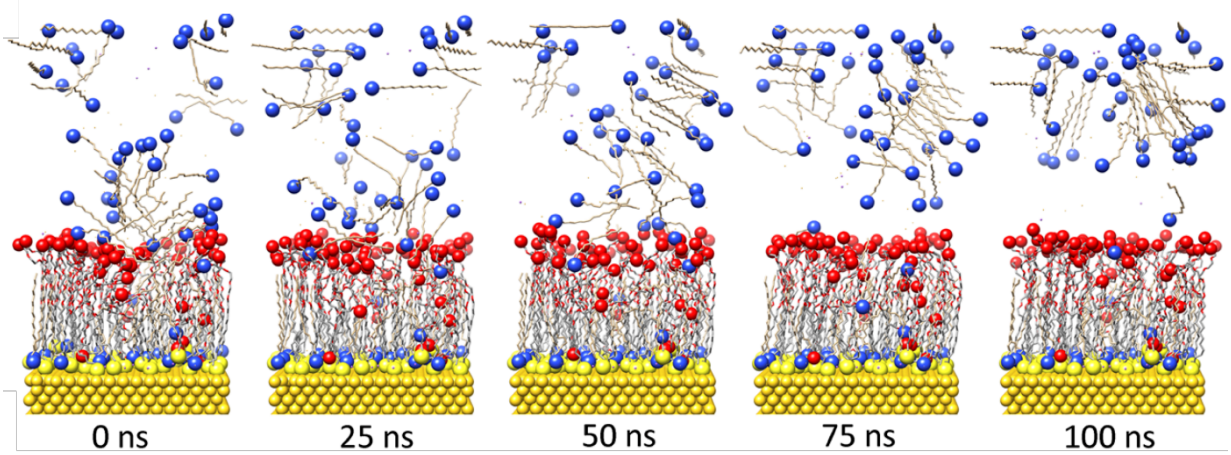

Figure S8. All-atom molecular dynamics of a CTAB micelle interacting with a MUHEG-functionalized Au (100) surface. Switching the solvent from water to pure EtOH at 0 ns leads to dissolution of the micelle and detachment of the charged surfactant molecules from the bound ligand layer.

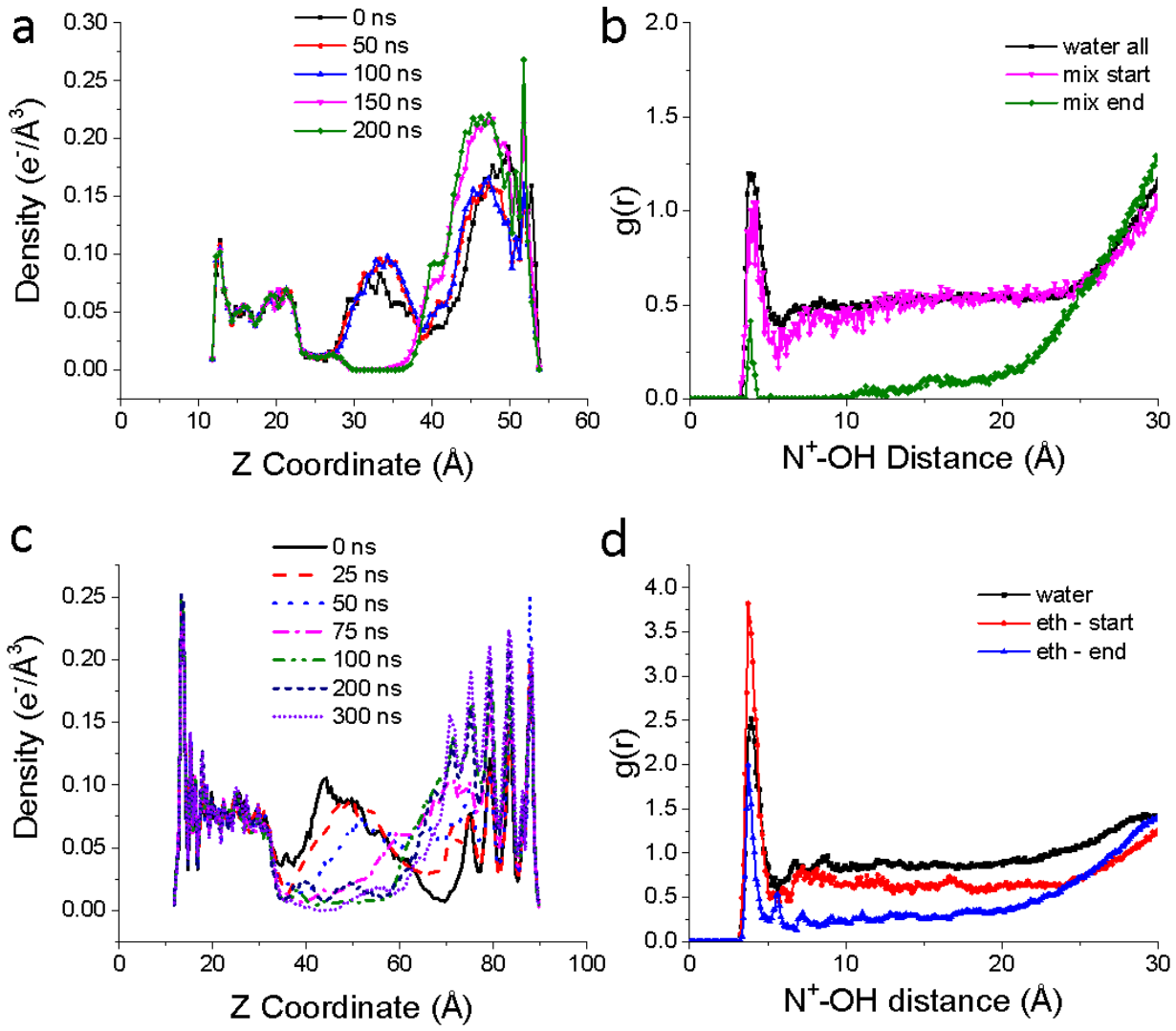

Figure S9. Electron density plots of CTA+ in the system(a,c), and radial distribution functions between the CTA+ ammonium and the terminal OH of MUHEG (b,d) in water and after transitioning to 52% (v/v) EtOH (a,b) or pure EtOH (c,d). In the radial distribution functions, "start" and "end" denote an average over the first and last 40 ns of the simulation trajectory.

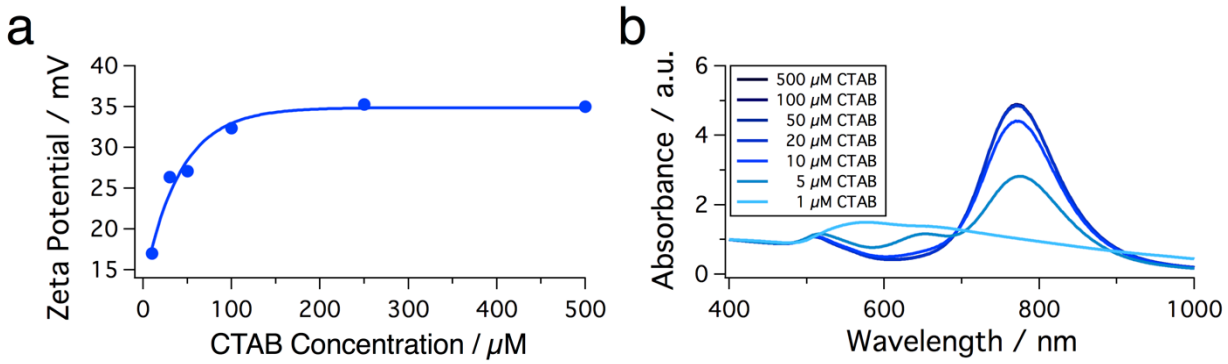

Figure S10. Impact of surfactant concentration on the colloidal stability of the MUHEG-coated gold nanorods. Zeta potential (a) and UV-vis spectra (b) of diluted dispersions show that only at extremely low CTAB concentrations (*i.e.* << 100 µM) the particles start to lose their positive surface charge and begin to agglomerate, which leads to a characteristic blue shift of the longitudinal LSPR due to AuNR side-by-side organisation.[14] The fitted line in (a) serves as a guide to the eye.

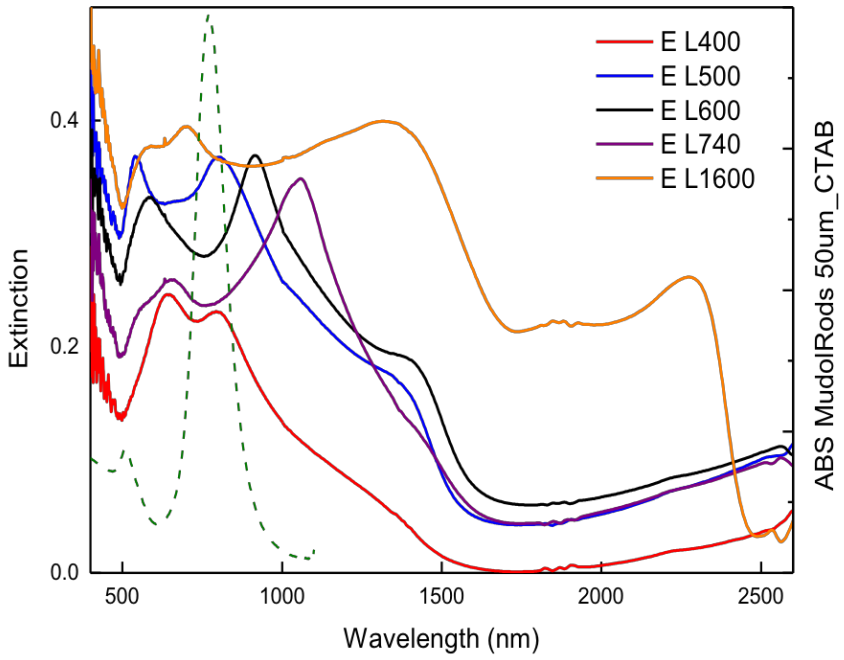

Figure S11. Extinction spectra of gold nanorod arrays with the square lattice parameter L varying from 400 nm to 1600 nm. The green dotted line corresponds to AuNRs dispersed in water. The values of the peak read-out from the spectra are listed in Table S2 below and compared for calculated positions of the diffraction peak occurring at the lattice dependent Rayleigh anomalies, assuming a refractive index of 1.55.

Table S2. Extinction peaks of AuNR square arrays.

Sample	Peak 1	Peak 2	Peak 3	Bragg SPP
L400	644 nm	844 nm	-	616 nm
L500	541 nm	803 nm	-	770 nm
L600	585 nm	916 nm	-	930 nm
L740	657 nm	1049 nm	-	1147 nm
L1600	703 nm	1326 nm	2276 nm	2480 nm

REFERENCES

(1) Scarabelli, L.; Grzelczak, M.; Liz-Marzán, L. M. Tuning Gold Nanorod Synthesis Through Prereduction with Salicylic Acid. *Chem. Mater.* **2013**, *25*, 4232–4238.

(2) Scarabelli, L.; Sánchez-Iglesias, A.; Perez-Juste, J.; Liz-Marzán, L. M. A "Tips and Tricks" Practical Guide to the Synthesis of Gold Nanorods. *J. Phys. Chem. Lett.* **2015**, *6*, 4270–4279.

(3) Qin, D.; Xia, Y.; Whitesides, G. M. Soft Lithography for Micro- and Nanoscale Patterning. *Nat. Protoc.* **2010**, *5*, 491–502.

(4) Matricardi, C.; Hanske, C.; Garcia-Pomar, J. L.; Langer, J.; Mihi, A.; Liz-Marzan, L. M. Gold Nanoparticle Plasmonic Superlattices as Surface-Enhanced Raman Spectroscopy Substrates. *ACS Nano* **2018**, *12*, 8531–8539.

(5) Abraham, M. J.; Murtola, T.; Schulz, R.; Páll, S.; Smith, J. C.; Hess, B.; Lindahl, E. GROMACS: High Performance Molecular Simulations Through Multi-Level Parallelism From Laptops to Supercomputers. *SoftwareX* **2015**, *1-2*, 19–25.

(6) Wright, L. B.; Rodger, P. M.; Corni, S.; Walsh, T. R. GolP-CHARMM: First-Principles Based Force Fields for the Interaction of Proteins with Au(111) and Au(100). *J. Chem. Theory Comput.* **2013**, *9*, 1616–1630.

(7) Huang, J.; MacKerell, A. D., Jr. CHARMM36 All-Atom Additive Protein Force Field: Validation Based on Comparison to NMR Data. *J. Comput. Chem.* **2013**, *34*, 2135–2145.

(8) Stillinger, F. H.; Rahman, A. Improved Simulation of Liquid Water by Molecular Dynamics. *J. Chem. Phys.* **1974**, *60*, 1545–1557.

(9) Colangelo, E.; Chen, Q.; Davidson, A. M.; Paramelle, D.; Sullivan, M. B.; Volk, M.; Levy, R. Experimental and Computational Investigation of the Structure of Peptide Monolayers on Gold Nanoparticles. *bioRxiv* **2016**, 083204.

(10) Hess, B.; Bekker, H.; Berendsen, H. J. C.; Fraaije, J. G. E. M. LINCS: a Linear Constraint Solver for Molecular Simulations. *J. Comput. Chem.* **1997**, *18*, 1463–1472.

(11) Darden, T.; York, D.; Pedersen, L. Particle Mesh Ewald: an N·Log(N) Method for Ewald Sums in Large Systems. *J. Chem. Phys.* **1993**, *98*, 10089–10092.

(12) Bussi, G.; Donadio, D.; Parrinello, M. Canonical Sampling Through Velocity Rescaling. *J. Chem. Phys.* **2007**, *126*, 014101.

(13) Pettersen, E. F.; Goddard, T. D.; Huang, C. C.; Couch, G. S.; Greenblatt, D. M.; Meng, E. C.; Ferrin, T. E. UCSF Chimera--a Visualization System for Exploratory Research and Analysis. *J. Comput. Chem.* **2004**, *25*, 1605–1612.

(14) Funston, A. M.; Novo, C.; Davis, T. J.; Mulvaney, P. Plasmon Coupling of Gold Nanorods at Short Distances and in Different Geometries. *Nano Lett.* **2009**, *9*, 1651–1658.